

Basic Principles in Modeling Adaptive Regulation and Immunodominance

Peter S. Kim, Peter P. Lee, and Doron Levy

1 Introduction

In this chapter we overview our recent work on mathematical models for the regulation of the primary immune response to viral infections and immunodominance. The primary immune response to a viral infection can be very rapid, yet transient. Prior to such a response, potentially reactive T cells wait in lymph nodes until stimulated. Upon stimulation, these cells proliferate for a limited duration and then undergo apoptosis or enter dormancy as memory cells. The mechanisms that trigger the contraction of the T cell population are not well understood. Immunodominance refers to the phenomenon in which simultaneous T cell responses against multiple target epitopes organize themselves into distinct and reproducible hierarchies. In many cases, eliminating the response to the most dominant epitope allows responses to subdominant epitopes to expand more fully. Likewise, if the two most dominant epitopes are removed, then the third most dominant response may expand. The mechanisms that drive immunodominance are also not well understood.

In order to understand the processes that control the T cells expansion and contraction, Mercado et al. demonstrated experimentally that the kinetics of CD8+ T cell expansion and contraction are determined within the first day of infection

P.S. Kim (✉)

School of Mathematics and Statistics, University of Sydney, NSW 2006, Australia
e-mail: P.Kim@maths.usyd.edu.au

P.P. Lee

Division of Hematology, Department of Medicine, Stanford University, Stanford, CA 94305, USA
e-mail: ppl@stanford.edu

D. Levy

Department of Mathematics and Center for Scientific Computation and Mathematical Modeling (CSCAMM), University of Maryland, College Park, MD 20742, USA
e-mail: dlevy@math.umd.edu

[20]. In another study of CD8+ T cell expansion, Kaech et al. showed that upon antigenic stimulation, naïve CD8+ T cells divide at least 7–10 times and differentiate into functional effector and memory cells even if antigen is removed [13]. An alternative experimental approach by van Stipdonk et al. also focused on CD8+ T cell stimulation [31]. They showed that naïve CD8+ T cells become activated after only 2 h of exposure to mature antigen-presenting cells (APCs). After activation, these T cells divided and differentiated into effector and eventually memory cells without a need for further antigenic stimulation. In a subsequent paper, they observed that naïve CD8+ T cells that have been stimulated for 20 h were able to carry out extensive proliferation and cytotoxic activity, characteristic of a fully developed immune response [30]. They proposed that the fate of a T cell response is governed by a “cell-intrinsic developmental program” that is set even before the first cell division takes place.

A couple of mathematical models of the T cell proliferation program have been developed in parallel to these experiments. Antia et al. devised a mathematical model to investigate whether the program is completely specified by the initial encounter with antigen or whether it can be subsequently modified by the amount of antigen present [1]. Their results favor the second paradigm in which the T cell population briefly expands in response to the amount of antigen present before committing to a fixed program. Wodarz and Thomsen [32] developed a mathematical model to find the optimal fixed program that could respond effectively to a wide variety of infections. They concluded that the 7–10 divisions observed experimentally represented such an optimum.

All together the experimental and mathematical modeling papers propose a general paradigm for T cell expansion, which can be stated as follows: upon stimulation, T cells enter a minimal developmental program of about 7–10 divisions that is followed by a period of antigen-dependent proliferation that terminates after a certain time or after a certain number of cell divisions.

While the precise mechanisms of immunodominance are not well understood, the majority of experimental and theoretical works agree on some form of T cell competition [4, 11, 14, 15, 22, 23]. The two most prevailing theories on the matter are that either T cells passively compete for a limited resource, most likely access to APCs, or that T cells actively suppress the development of other T cells.

Our approach to deriving a mathematical model of immunodominance is based on extending the adaptive regulation model to consider the case of multiple, simultaneous T cell responses. This point of view implies that immunodominance may occur as a natural result of the iTreg-mediated contraction of the T cell response proposed in [17].

Several mathematical models for immunodominance have been developed in the literature. Here we mention several key works and refer to [16] for a more complete overview of these works and their results. De Boer and Perelson show that for each target epitope only the T cell clone with the highest affinity will survive long-term T cell competition [7, 8]. Nowak develops a mathematical model and predicts that for an antigenically homogeneous virus population, the immune response will ultimately be directed against only one epitope, a situation known as complete

immunodominance [21]. De Boer et al. formulate a mathematical model to analyze experimental measurements of the CD8+ T cell response to lymphocytic choriomeningitis virus [10]. The response consists of one immunodominant response and one subdominant response against different epitopes. De Boer et al. propose that differences in growth rate and recruitment times of different T cell populations can account for immunodominance. Antia et al. also formulate a model in which multiple epitope-specific T cell populations undergo a brief period of expansion in response to antigen, followed by a period of antigen-independent proliferation and contraction [1]. Handel and Antia develop a mathematical model to explain the shift in the immunodominance hierarchy between the primary and secondary responses to influenza A [12]. Scherer et al. present an alternative mathematical model in which the down-modulation of antigen-presentation leads to long-term coexistence of T cell responses [25]. A related work by Scherer et al. is an agent-based model to understand whether T cells compete for nonspecific stimuli, such as access to the surface of APCs, or for specific stimuli, such as MHC:epitope complexes [27].

Our main goal in developing mathematical models for the primary immune response and immunodominance is to identify at least some of the main mechanisms by which the primary immune response is regulated and by which immunodominance emerges. After carefully studying other approaches, we developed mathematical models that are based on the following basic principles:

1. The primary immune response should be adaptively controlled. This adaptive process can work in combination with any proliferation preprograms.
2. The adaptive control is conducted by regulatory cells. The number of regulatory cells cannot be directly proportional to the total number of effector cells as the body has no way of keeping track of this number. Instead, the process should depend only on the dynamics of individual cells.
3. Immunodominance is a by-product of adaptive regulation. Adaptive regulatory cells, which are created in an epitope-specific way, can then regulate the system in a nonspecific fashion.

When it comes to adaptive regulation, our main observation in [17] was that the preprogram paradigm as is, is inconsistent with the experimental data of Badovinac et al. [2], which showed that a 10,000-fold difference in antigen-specific naïve T cell concentrations only led to a 13-fold higher peak in the effector response. Any mechanism that relies only on a preprogrammed cell division must scale linearly with the precursor frequencies. This led us to derive a mathematical model that is based on adaptive regulatory T cells (iTregs). Our hypothesis is that T cell responses are adaptively regulated in a process that results from the dynamics of immune cells that interact based on relatively simple rules. Following the same line of thought, our model of immunodominance from [16] is based on considering immunodominance as a by-product of the regulated T cell contraction. It is sufficient to add a single rule to the model of adaptive regulation to explain immunodominance.

The model in [16] represents an “extended” model that divides T cells into helper (CD4)+ and killer (CD8+) subpopulations and considers interactions among helper T cells, killer T cells, and iTregs. This model has the advantage of presenting a more

encompassing view of immune interactions; however, its complexity obfuscates the key feedback loop that drives the expansion and contraction of a primary T cell response and the development of immunodominance.

To gain insight into regulatory mechanisms, we will begin by presenting a simplified model that elucidates the key feedback loop, while still capturing the qualitative behavior of the extended model from [16]. The primary simplification is that the helper and killer subpopulations are considered as a collective population of effector T cells, since the expansion and contraction of helper and killer T cells occur roughly in parallel [9]. In this manner, the simplified model focuses on the negative feedback between the effector and regulatory T cell populations. Using the simplified model, we will discuss insights that are difficult to obtain using the extended model.

The structure of this chapter is as follows. In Sect. 2 we present our mathematical models of adaptive regulatory T cell-mediated contraction. First, in Sect. 2.1 we present the simplified model of adaptive regulation, a model that does not separate helper and killer T cells. This model is taken from [17]. The model is extended to include helper T cells in Sect. 2.2. Mathematical models of immunodominance are described in Sect. 3. The models of immunodominance are based on the models of adaptive regulation and follow the same pattern of presentation: we start in Sect. 3.1 with the basic model of immunodominance that does not include helper T cells. This model is the original model we proposed, a model that has not yet been published. We then continue in Sect. 3.2 with the extended model that includes helper T cells. This model was published in [16]. Numerical results are given in Sect. 4. We show some results for the adaptive regulation model, results that demonstrate the robustness of the system to small perturbations in the precursor frequencies. We then continue in Sect. 4.2 with simulations of both immunodominance models, focusing on results that were obtained with the simple model. A discussion and concluding remarks are provided in Sect. 5.

2 Mathematical Model of Adaptive Regulatory T cell-Mediated Contraction

In this section we overview our models for adaptive regulatory T cell-mediated contraction. We start in Sect. 2.1 with the basic adaptive regulation model we introduced in [17]. This model is based on the hypothesis that primary response may be governed by a feedback control system involving adaptive regulatory cells (iTregs) rather than by intrinsic, intracellular feedback mechanisms.

In Sect. 2.2 we extend the adaptive regulation model of Sect. 2.1 to a more comprehensive model that includes helper T cells and positive growth signals. While this model better adheres to the biology when compared with the basic model in Sect. 2.1, the basic principle that enables that contraction of the immune response remains the same: adaptive regulatory cells provide the required negative feedback to generate the desired contraction.

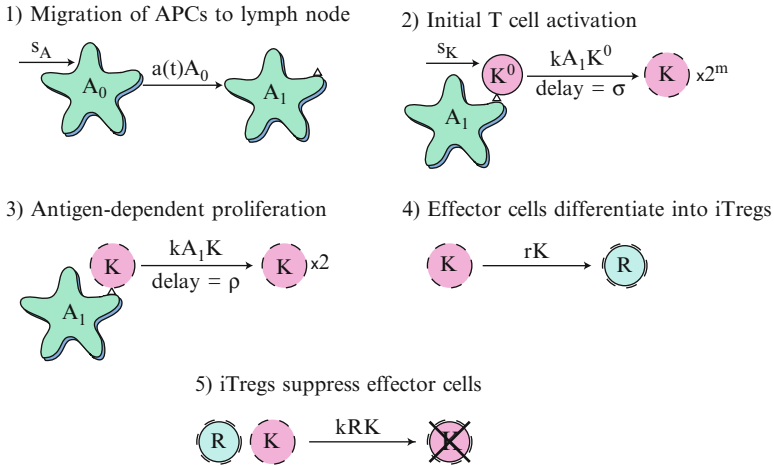


Fig. 1 Diagram of the iTreg model. (1) Immature APCs pick up antigen at the site of infection at a time-dependent rate $a(t)$. These APCs mature and migrate to the lymph node. (2) Mature antigen-bearing APCs present antigen to naïve T cells causing them to activate and enter the minimal developmental program of m divisions. (3) Effector cells that have completed the minimal program continue to divide upon further interaction with mature APCs. (4) Effector cells differentiate into iTregs at rate r . (5) The iTregs suppress effector cells. Although not indicated, each cell in the diagram has a natural death rate

In both models, the number of regulatory cells is dynamically controlled. A certain ratio of the effector cells are converted into regulatory cells. Such a process is postulated to be controlled on the level of the individual cell possibly even in a probabilistic way. There is no need for a central control of the number of regulatory cells that depends on the total number of effector cells. Such a mechanism would be biologically irrelevant. The precise means by which some of the effector cells turn into regulatory cells is irrelevant for the present work. It is possible that asymmetric differentiation is involved, or perhaps effector cells actually change their trait. In any event, all that matters is that a certain fraction of the effector cells will eventually turn into regulatory cells, due to a local process on the level of the individual cell.

2.1 Mathematical Model of Adaptive Regulation: Feedback Loop

We start with the simple model for monoclonal T cell responses taken from [17]. This model can be summarized in five steps (illustrated in Fig. 1):

1. APCs mature, present relevant target antigen, and migrate from the site of infection to the draining lymph node.

2. In the lymph node, APCs activate naïve T cells that enter a minimal developmental program of m cell divisions.
3. T cells that have completed the minimal developmental program become effector cells that keep dividing in an antigen-dependent manner as long as they are not suppressed by iTregs.
4. Effector cells differentiate into iTregs at a constant rate.
5. The iTregs suppress effector cells upon interaction.

For convenience, we group the entire T cell population into one unit consisting of both CD4+ and CD8+ T cells. This assumption simplifies the model and focuses on the feedback loop between effector cells and iTregs. This simplification does not capture the heterogeneous roles of CD4+ and CD8+ T cells in driving and regulating the overall T cell response. In particular, CD4+ T cells are the primary secreters of the cytokine interleukin-2 (IL-2), which drives T cell proliferation. In addition, nonregulatory CD4+ T cells are the major, if not only, source of iTregs generated in the periphery [24]. On the other hand, CD8+ T cells proliferate more rapidly and extensively than CD4+ T cells and also exhibit cytotoxic activity [9]. To capture these differences, we develop a more extensive model that includes separate CD4+ and CD8+ subpopulations in Sect. 2.2.

In addition, we assume that iTregs do not undergo further proliferation after differentiating from effector T cells. As with the previous assumption, this simplification also allows the model to focus on the feedback loop between effector cells and iTregs without incorporating an additional positive stimulation of iTreg via APCs. We also remove this simplification in the extended model of Sect. 2.2.

The T cell dynamics in the model are based on the concept of antigen-independent T cell proliferation and contraction. Various experiments have shown that during a primary CD8+ T cell response, T cell kinetics are determined early on (after approximately 24 h of stimulation) [20], T cell expansion and differentiation are antigen-independent after initial exposure (approximately 20 h of stimulation) [30], and T cells divide at least 7–10 times after stimulation even if antigen is removed [13]. Similar results have been found for CD4+ T cells [33]. These results along with other related studies have led to the notion of *antigen-independent T cell program*. The main principle is that following initial stimulation, the primary T cell response is governed by an independent *program* that is insensitive to the nature and duration of subsequent antigen stimulation. The implication is that T cells somehow regulate themselves during a primary response without feedback from the antigen source. Since in this chapter we only consider immunodominance during a primary T cell response, we model T cell dynamics from the perspective of an antigen-independent, self-regulating process. Other examples of mathematical models of antigen-independent primary T cell response dynamics can be found in Antia et al. and Wodarz et al. [1, 32].

The mathematical model corresponding to Fig. 1 is formulated as the following system of delayed differential equations (DDEs):

$$\dot{A}_0(t) = s_A - d_0 A_0(t) - a(t) A_0(t), \quad (1)$$

$$\dot{A}_1(t) = a(t)A_0(t) - d_1A_1(t), \quad (2)$$

$$\dot{K}^0(t) = s_K - \delta_0K^0(t) - kA_1(t)K^0(t), \quad (3)$$

$$\begin{aligned} \dot{K}(t) = & 2^m kA_1(t - \sigma)K^0(t - \sigma) - kA_1(t)K(t) + 2kA_1(t - \rho)K(t - \rho) \\ & - (\delta_1 + r)K(t) - kR(t)K(t), \end{aligned} \quad (4)$$

$$\dot{R}(t) = rK(t) - \delta_1R(t). \quad (5)$$

Here, A_0 is the concentration of APCs at the site of infection, A_1 is the concentration of APCs that have matured, started to present target antigen, and migrated to the lymph node, K^0 is the concentration of naïve T cells in the lymph node, K is the concentration of effector cells, and R is the concentration of iTregs.

Equation (1) pertains to APCs waiting at the site of infection. These cells are supplied at a constant rate s_A and die at a proportional rate d_0 . Without stimulation, the population remains at its equilibrium level, s_A/d_0 . The time-dependent coefficient $a(t)$ is the rate of APC stimulation from antigen at the site of infection. Equation (2) pertains to APCs that have matured, started to present relevant antigen, and migrated to the lymph node. The first term of the equation corresponds to the rate at which these APCs enter the lymph node. The second term is the natural death rate of this population.

Equation (3) pertains to naïve T cells. This population is replenished at a constant rate s_K and dies at a proportional rate δ_0 . Without stimulation, the population remains at its equilibrium level, s_K/δ_0 . The third term in this equation is the rate of stimulation of naïve T cells by mature APCs. The bilinear form of this term follows the law of mass action where k is the proportionality constant (or kinetic coefficient).

Equation (4) pertains to effector cells. The first term gives the rate at which activated naïve T cells enter the effector state after finishing the minimal developmental program. This term is similar to the last term of Eq. (3), except that it has an additional coefficient of 2^m and it depends on cell concentrations at time $t - \sigma$. The coefficient 2^m accounts for the increase in population of naïve T cells after m divisions, and the time delay σ is the duration of the minimal developmental program. The second term is the rate at which effector cells are stimulated by mature APCs for further division, and the third term is the rate in which cells reenter the effector population after having divided once. The fourth term is the rate that effector cells exit the population through death at rate δ_1 or differentiation into iTregs at rate r . The final term is the rate that effector cells are suppressed by iTregs. We assume that the rate of iTreg–effector interactions follows the same mass action law as APC–T cell interactions.

Equation (5) pertains to iTregs. The first term is the rate at which effector cells differentiate into iTregs, and the second term is the rate at which iTregs die. We assume that iTregs have the same death rate as effector cells.

The parameter estimates used for this model are taken from [17] and are summarized in Table 1. For the function $a(t)$, representing the rate of antigen

Table 1 Estimates for model parameters

Parameter	Description	Estimate
$A_0(0)$	Initial concentration of immature APCs	10
$K^0(0)$	Initial concentration of naïve T cells	0.04
d_0	Death/turnover rate of immature APCs	0.03
d_1	Death/turnover rate of mature APCs	0.8
δ_0	Death/turnover rate of naïve T cells	0.03
δ_1	Death/turnover rate of effector T cells	0.4
s_A	Supply rate of immature APCs	$d_0 A_0(0) = 0.3$
s_K	Supply rate of naïve T cells	$\delta_0 K^0(0) = 0.0012$
k	Kinetic coefficient	20
m	# of divisions in minimal developmental program	7
n	Maximum number of antigen-dependent divisions	3 to 10
ρ	Duration of one T cell division	1/3
σ	Duration of minimal developmental program	$1 + (m - 1)\rho = 3$
$a(t)$	Rate of APC stimulation	Eq. (6)
b	Duration of antigen availability	10
c	Level of APC stimulation	1
r	Rate of differentiation of effector cells into iTregs	0.01

Concentrations are in units of $k/\mu\text{L}$, and time is measured in days

stimulation, we assume that it starts at 0, remains positive for some time, and eventually returns to 0. To generate a smooth function for $a(t)$, we let

$$\phi(x) = \begin{cases} e^{-1/x^2}, & \text{if } x \geq 0, \\ 0, & \text{if } x < 0, \end{cases}$$

and set

$$a(t) = c \frac{\phi(t)\phi(b-t)}{\phi(b)^2}, \quad (6)$$

where $b, c > 0$. The variable t is defined such that mature APCs begin appearing in the lymph node at $t = 0$, although the infection may have begun slightly earlier. We estimate that the duration of antigen availability, b , is about 10 days. Furthermore, we estimate that the level of APC stimulation, c , is around 1. (See Fig. 2 for graphs of $a(t)$ for $b = 3$ and $b = 10$ when $c = 1$.)

2.2 *Extended Model of Adaptive Regulation: Helper and Killer T Cells*

The mathematical model presented in this section is an extension of the model in Sect. 2.1. The main extension of the model is to separate the nonregulatory

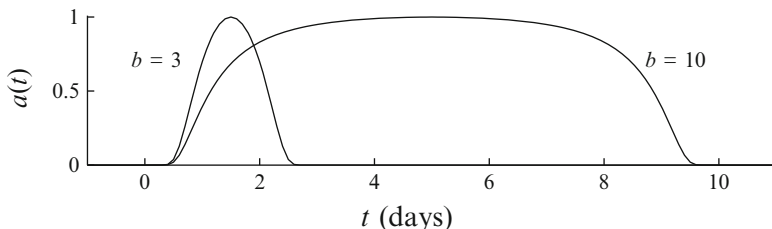


Fig. 2 Graphs of the antigen function $a(t)$ given by Eq. (6) for $b = 3$ and $b = 10$ when $c = 1$. The function $a(t)$ represents the time-dependent rate that immature APCs pick up antigen and are stimulated

T cell population into CD4+ and CD8+ T cells. CD4+ T cells are the primary producers of positive growth signal, particularly IL-2, and CD8+ T cells are the main proliferators. Furthermore, iTregs differentiate from effector CD4+ cells and suppress both effector CD4+ and CD8+ cells [24]. The extended model can be summarized in six steps (illustrated in Fig. 3):

1. APCs mature, present relevant target antigen, and migrate from the site of infection to the draining lymph node.
2. In the lymph node, APCs activate naïve CD4+ and CD8+ T cells that enter a minimal developmental program of m_1 or m_2 cell divisions, respectively.
3. Effector CD4+ and CD8+ T cells both secrete positive growth signal at different rates.
4. CD4+ and CD8+ T cells that have completed the minimal developmental program become effector cells that keep dividing as long as they are not suppressed by iTregs.
 - CD4+ T cells proliferate in response to interactions with APCs (It is assumed that CD4+ T cells produce enough IL-2 to stimulate their own growth in an autocrine loop. Hence, we do not explicitly model the secretion and consumption of IL-2 by CD4+ T cells.).
 - CD8+ T cells proliferate after consuming free positive growth signal.
5. During the immune response, some effector CD4+ T cells differentiate into iTregs.
6. The iTregs suppress effector CD4+ and CD8+ T cells and proliferate after consuming free positive growth signal.

The mathematical model corresponding to Fig. 3 is formulated as the following system of DDEs:

$$\dot{A}_0(t) = s_A - d_0 A_0(t) - a(t) A_0(t), \quad (7)$$

$$\dot{A}_1(t) = a(t) A_0(t) - d_1 A_1(t), \quad (8)$$

$$\dot{H}^0(t) = s_H - \delta_0 H^0(t) - k A_1(t) H^0(t), \quad (9)$$

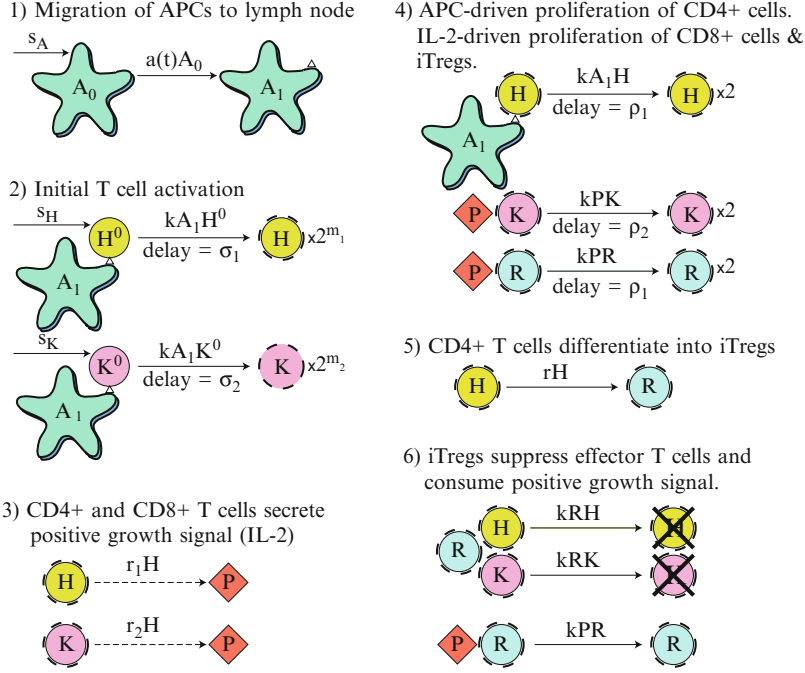


Fig. 3 Diagram of the extended adaptive iTreg model. (1) Immature APCs pick up antigen at the site of infection at a time-dependent rate $a(t)$. These APCs mature and migrate to the lymph node. (2) Mature antigen-bearing APCs present antigen to naïve CD4+ and CD8+ T cells causing them to activate and enter the minimal developmental program of m_1 and m_2 divisions, respectively. (3) Effector CD4+ and CD8+ T cells secrete positive growth signals at different rates. (4) CD4+ and CD8+ T cells that completed the minimal program become effector cells and continue to divide. CD4+ T cells proliferate upon further interaction with mature APCs. CD8+ T cells and iTregs proliferate after consuming positive growth signal. (5) Effector CD4+ T cells differentiate into iTregs at a constant rate. (6) The iTregs suppress effector CD4+ and CD8+ T cells. Although not indicated, each cell in the diagram has a natural death rate

$$\dot{H}(t) = 2^{m_1}kA_1(t - \sigma_1)H^0(t - \sigma_1) - kA_1(t)H(t) + 2kA_1(t - \rho_1)H(t - \rho_1) - (\delta_H + r)H(t) - kR(t)H(t), \quad (10)$$

$$\dot{K}^0(t) = s_K - \delta_0K^0(t) - kA_1(t)K^0(t), \quad (11)$$

$$\dot{K}(t) = 2^{m_2}kA_1(t - \sigma_2)K^0(t - \sigma_2) - kP(t)K(t) + 2kP(t - \rho_2)K(t - \rho_2) - \delta_KK(t) - kR(t)K(t), \quad (12)$$

$$\dot{P}(t) = r_1H(t) + r_2K(t) - \delta_PP(t) - kP(t)K(t) - kP(t)R(t), \quad (13)$$

$$\dot{R}(t) = rH(t) - kP(t)R(t) + 2kP(t - \rho_1)R(t - \rho_1) - \delta_RR(t). \quad (14)$$

As in Sect. 2.1, A_0 is the concentration of APCs at the site of infection and A_1 is the concentration of APCs that have matured, started to present target antigen, and

migrated to the lymph node. The variable H^0 is the concentration of naïve CD4+ killer T cells, H is the concentration of effector CD4+ cells, K^0 is the concentration of naïve CD8+ (killer) T cells, K is the concentration of effector CD8+ cells, and R is the concentration of iTregs. In addition, P is the concentration of positive growth signal (e.g., IL-2).

Equations (7) and (8) are identical to Eqs. (1) and (2) in Sect. 2.1. Equations (9) and (11) pertain to naïve CD4+ and CD8+ T cells, respectively. The CD4+ and CD8+ populations are replenished at constant rates s_H and s_K , respectively, and die at a proportional rate δ_0 . The third terms in Eqs. (9) and (11) are the rates of stimulation of naïve CD4+ and CD8+ T cells by mature APCs. The bilinear form of this term follows the law of mass action where k is the proportionality constant (or kinetic coefficient). We assume that all cell–cell or cell–signal interactions follow the same law of mass action.

Equation (10) pertains to effector CD4+ cells. The first term gives the rate at which activated naïve CD4+ T cells enter the effector state after finishing the minimal developmental program of m_1 cell divisions. The time delay σ_1 is the duration of the minimal developmental program. The second term is the rate at which effector CD4+ cells are stimulated by mature APCs for further division, and the third term is the rate in which cells reenter the effector CD4+ population after having divided once. The time delay ρ_1 is the duration of one CD4+ cell division. The fourth term is the rate at which effector CD4+ cells exit the population through death at rate δ_H or differentiation into iTregs at rate r . The final term is the rate at which effector CD4+ cells are suppressed by iTregs.

Equation (12) pertains to effector CD8+ cells. The first term gives the rate at which activated naïve CD8+ T cells enter the effector state after finishing the minimal developmental program of m_2 cell divisions. The time delay σ_2 is the duration of the minimal developmental program. The second term is the rate at which effector CD8+ cells are stimulated by positive growth signal for further division, and the third term is the rate at which cells reenter the effector CD8+ population after having divided once. The time delay ρ_2 is the duration of one CD8+ cell division. The fourth term is the rate at which effector CD8+ cells die at rate δ_K . The final term is the rate at which effector CD8+ cells are suppressed by iTregs.

Equation (13) pertains to positive growth signal. The first two terms are the rates at which positive growth signal is secreted by effector CD4+ and CD8+ cells, respectively. The third term is the decay rate of positive growth signal. The fourth and fifth terms are the rates at which positive growth signal is consumed by effector CD8+ cells and iTregs, respectively.

Equation (14) pertains to iTregs. The first term is the rate at which effector CD4+ cells differentiate into iTregs. The second term is the rate at which iTregs are stimulated by positive growth signal for further division, and the third term is the rate at which cells reenter the iTreg population after having divided once. The time delay ρ_1 is the duration of one CD4+ cell division. The fourth term is the rate at which iTregs die. We assume that iTregs have the same division time and death rate as CD4+ cells.

Table 2 Estimates for additional parameters used in the extended model

Param.	Description	Estimate
δ_H	Death/turnover rate of effector CD4+ T cells	0.23
δ_K	Death/turnover rate of effector CD8+ T cells	0.4
$H^0(0)$	Initial naïve CD4+ T cell concentration	see Scenario 2
$K^0(0)$	Initial naïve CD8+ T cell concentration	see Scenario 2
s_H	Supply rate of naïve CD4+ T cells	$\delta_0 H^0(0)$
s_K	Supply rate of naïve CD8+ T cells	$\delta_0 K^0(0)$
m_1	# of divisions in minimal CD4+ developmental program	2
m_2	# of divisions in minimal CD8+ developmental program	7
ρ_H	Duration of one T cell division	11/24
ρ_K	Duration of one T cell division	1/3
σ_H	Duration of min developmental program: $1 + (m_H - 1)\rho_H$	1.46
σ_K	Duration of min developmental program: $1 + (m_K - 1)\rho_K$	3
r_1	Rate of secretion of positive growth signal by CD4+ cells	100
r_2	Rate of secretion of positive growth signal by CD8+ cells	1
δ_P	Decay rate of free positive growth signal	5.5
r	Rate of differentiation of effector cells into iTregs	0.02

Other parameters are the same as those used in Table 1 for the simplified model

Concentrations are in units of k/ μ L, and time is measured in days

In this model, we use the same parameters as in Table 1 for the simplified model, except for those listed in Table 2. We assume that CD4+ and CD8+ T cells have halflives of 3 days and 41 h, respectively, yielding death rates of $\delta_H = 0.23$ and $\delta_K = 0.4/\text{day}$ [9]. We assume that CD4+ and CD8+ populations have doubling times of 11 h and 8 h, respectively, yielding cell division rates of $\rho_H = 11/24$ and $\rho_K = 1/3$ day [9]. We do not have good estimates of the secretion rates of positive growth signal by effector T cells, hence we estimate that CD4+ and CD8+ T cells secrete growth signal at rates $r_1 = 100$ and $r_2 = 1/\text{day}$, respectively. We assume that free positive growth signal decays with a half-life of 3 h, yielding an estimate of $\delta_P = 5.5/\text{day}$. In this model only effector CD4+ T cells can differentiate into iTregs, so the new estimate of the iTreg differentiation rate, r , must be higher than the previous estimate of $r = 0.01/\text{day}$ to maintain similar dynamics. Hence, in this model, we set $r = 0.03/\text{day}$.

3 Mathematical Models of Immunodominance

In this section we explain how to expand our model for monoclonal T cell responses to polyclonal responses. We show that the expanded model automatically recreates elements of the characteristic behavior associated with immunodominance. In this way, we demonstrate that immunodominance may occur as a natural result of iTreg-mediated self-regulation of polyclonal T cell responses.

We begin in Sect. 3.1 with deriving a basic immunodominance model that demonstrated immunodominance as an extension of the basic model of adaptive regulation. We then continue in Sect. 3.2 with an extended model of

immunodominance. This extended immunodominance model is the model published in [16]. The basic immunodominance model is new. While the basic model is less accurate from a biological point of view, it still captures the main principles on which the extended model is based.

3.1 A Basic Model

We extend the model from Sect. 2.1 to polyclonal T cell responses. The model includes n T cell clones that react to mature antigen-bearing APCs at different rates, k_i . The model is formulated as the following system of DDEs:

$$\dot{A}_0(t) = s_A - d_0 A_0(t) - a(t) A_0(t), \quad (15)$$

$$\dot{A}_1(t) = a(t) A_0(t) - d_1 A_1(t), \quad (16)$$

$$\dot{K}_i^0(t) = s_{K,i} - \delta_0 K_i^0(t) - k_i A_1(t) K_i^0(t), \quad (17)$$

$$\begin{aligned} \dot{K}_i(t) = & 2^m k_i A_1(t - \sigma) K_i^0(t - \sigma) - k_i A_1(t) K_i(t) + 2k_i A_1(t - \rho) K_i(t - \rho) \\ & - (\delta_1 + r) K_i(t) - k R_{\text{total}}(t) K_i(t), \end{aligned} \quad (18)$$

$$\dot{R}_i(t) = r K_i(t) - \delta_1 R_i(t), \quad (19)$$

where $R_{\text{total}} = \sum R_i$ and $i = 1, \dots, n$. As before, A_0 is the concentration of immature APCs at the site of infection, and A_1 is the concentration of mature antigen-bearing APCs in the lymph node. The variables K_i^0 , K_i , and R_i are the concentrations of naïve, effector, and regulatory T cells with specificity $\#i$.

Equations (15) and (16) for the APCs are identical to Eqs. (1) and (2). Equations (17)–(19) are analogous to Eqs. (3)–(5), except that each T cell clone is supplied at a different rate $s_{N,i}$, has its own kinetic coefficient k_i , and effector cells can be suppressed by any regulatory cell, independent of their origin. The supply rate, $s_{K,i}$, of T cell clones is related to the initial concentration of that clonal population by $s_{K,i} = d_1 K_i^0(0)$. From the estimates in [17], the kinetic coefficient $k_i = p_i k_0$, where $k_0 = 40$ and p_i is the probability that T cells of the i th clone react to antigens presented on the APCs. All other parameters are taken from Table 1.

3.2 An Extended Immunodominance Model: Including the Helper T Cells

Following the basic principle of the model in Sect. 3.1, we extend the mathematical model of Sect. 2.2 to polyclonal T cell responses. The model includes n clones that react to mature antigen-bearing APCs at different rates, k_i , and is formulated as the following system of DDEs:

$$\dot{A}_0(t) = s_A - d_0 A_0(t) - a(t) A_0(t), \quad (20)$$

$$\dot{A}_1(t) = a(t)A_0(t) - d_1A_1(t), \quad (21)$$

$$\dot{H}_i^0(t) = s_{H,i} - \delta_0H_i^0(t) - k_iA_1(t)H_i^0(t), \quad (22)$$

$$\begin{aligned} \dot{H}_i(t) = & 2^{m_1}k_iA_1(t - \sigma_1)H_i^0(t - \sigma_1) - k_iA_1(t)H_i(t) + 2k_iA_1(t - \rho_1)H_i(t - \rho_1) \\ & - (\delta_H + r)H_i(t) - kR_{\text{total}}(t)H_i(t), \end{aligned} \quad (23)$$

$$\dot{K}_i^0(t) = s_{K,i} - \delta_0K_i^0(t) - k_iA_1(t)K_i^0(t), \quad (24)$$

$$\begin{aligned} \dot{K}_i(t) = & 2^{m_2}k_iA_1(t - \sigma_2)K_i^0(t - \sigma_2) - kP(t)K_i(t) + 2kP(t - \rho_2)K_i(t - \rho_2) \\ & - \delta_KK_i(t) - kR_{\text{total}}(t)K_i(t), \end{aligned} \quad (25)$$

$$\dot{P}(t) = r_1H_{\text{total}}(t) + r_2K_{\text{total}}(t) - \delta_PP(t) - kP(t)K_{\text{total}}(t) - kP(t)R_{\text{total}}(t), \quad (26)$$

$$\dot{R}_i(t) = rH_i(t) - kP(t)R_i(t) + 2kP(t - \rho_1)R_i(t - \rho_1) - \delta_HR_i(t). \quad (27)$$

Here $H_{\text{total}} = \sum H_i$, $K_{\text{total}} = \sum K_i$, and $R_{\text{total}} = \sum R_i$ for $i = 1, \dots, n$. As in Sect. 2.2, A_0 is the concentration of APCs at the site of infection and A_1 is the concentration of APCs that have matured, started to present target antigen, and migrated to the lymph node. For each clone i , the variable H_i^0 is the concentration of naïve CD4+ (helper) T cells, H_i is the concentration of effector CD4+ cells, K_i^0 is the concentration of naïve CD8+ (helper) T cells, and K_i is the concentration of effector CD8+ cells, and R_i is the concentration of iTregs. Finally, P is the concentration of positive growth signal.

Equations (20) and (21) are identical to Eqs. (7) and (8). Equations (22), (24), and (27) describe the dynamics of the naïve CD4+ T cells, naïve CD8+ T cells, and regulatory cells, respectively, for each clone i . These equations are identical to Eqs. (9), (11), and (14).

The assumption about the nonspecific suppression of the activated CD4+ and CD8+ T cells is encoded into the model in Eqs. (23) and (25). The last term in both equations shows that the suppression of the activated cells is done using the iTregs that originated from all clones.

Finally, the dynamics of the positive growth signal is proportional to the total population sizes of the activated CD4+ and CD8+ T cells, as well as the total number of iTregs in the system.

4 Results

In this section we present results obtained by simulating the mathematical model from Sects. 2 and 3. We start in Sect. 4.1 with simulations of the basic model of adaptive regulation. We focus our attention on demonstrating the robustness of the model to large variations in precursor frequencies. Additional simulations of this model can be found in [17]. In Sect. 4.2 we present simulations of the immunodominance models. Most of the simulations are of the basic model

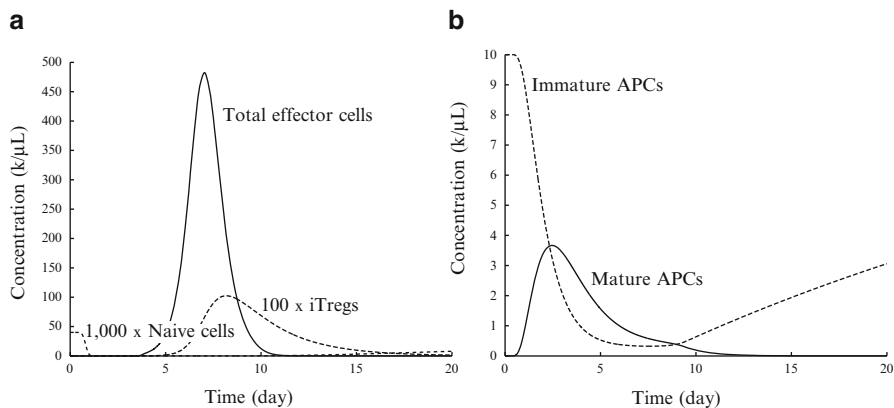


Fig. 4 Time evolution of immune cell populations. (a) The dynamics of naïve, effector, and regulatory T cells over 20 days. (b) The dynamics of immature and mature APCs

from Sect. 3.1. We provide one example of simulations of the extended model from Sect. 3.2. Additional simulations of the extended model can be found in [16].

4.1 Adaptive Regulation: Numerical Simulations

We start by numerically solving Eqs. (1)–(5). The model parameters are set according to Table 1. The simulations are done using the DDE solver “dde23” in MATLAB R2008a. The time evolution of the different cell populations is shown in Fig. 4.

It is evident from Fig. 4 that nearly all available antigen-specific naïve T cells are recruited within a day of antigen presentation, a result corroborated by the experimental data of [20]. In addition, the effector cell and mature APC populations peak at day 7.0 and day 2.5. In our model, the variable t corresponds to the time after antigen presentation begins in the lymph node. This event occurs approximately one day after infection [3]. Hence, our simulated measurements translate to T cell and APC peaks at day 8.0 and day 3.5 after infection. These results coincide well with the experimental measurements that the T cell and APC populations peak at around day 8 and day 3.2 after infection (see [3, 9]).

Figure 5a displays phase portraits of the iTreg versus the effector population for initial naïve cell concentrations of 0.0004, 0.004, 0.04, 0.4, and 4k/μL. The five curves correspond to population doublings of 18.4, 15.9, 13.6, 11.3, and 9.1, respectively, showing that every tenfold increase or decrease in precursor concentrations corresponds to approximately 2.2 fewer or 2.2 additional divisions that adjust the difference. Thus, larger initial conditions lead to larger T cell responses, but not at the level of sensitivity exhibited by the two program-based

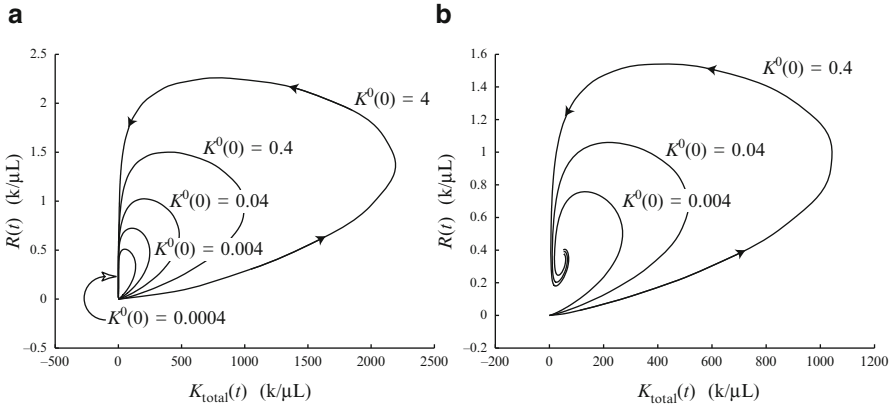


Fig. 5 Phase portraits of iTreg versus effector dynamics over 20 days. **(a)** Five different precursor frequencies, $K^0(0) = 0.0004, 0.004, 0.04, 0.4,$ and $4\text{k}/\mu\text{L}$. The curve for $K^0(0) = 0.04$ corresponds to Fig. 4. **(b)** T cell dynamics under persistent antigen stimulation, i.e., $b = 1,000$ days for three different precursor frequencies, $K^0(0) = 0.004, 0.04,$ and $0.4\text{k}/\mu\text{L}$.

models. All phase portraits exhibit similar shapes and return to the resting state in a timely fashion. The phase portraits represent the dynamics over 20 days as in Fig. 4.

Figure 5b shows similar phase portraits as in Fig. 5a, except that the duration, b , of antigen presentation is set to 1,000 days so that antigen is chronically presented. The figure shows that the effector and iTreg populations spiral into a stable fixed point. The elongated shapes form as a result of the rapid increase in the level of antigen presentation by mature APCs over the first few days after infection before decaying to a steady level several days later. The brief burst of mature APC levels in the lymph node allows the effector concentration to expand rapidly for a brief time before being attracted to the stable fixed point.

4.2 Immunodominance: Numerical Simulations

We start by showing results that were obtained from simulating the basic immunodominance model from Sect. 3.2. We numerically simulate solutions to Eqs. (15)–(19). The numerical solution is obtained using the DDE solver “dde23” in MATLAB R2008a. We consider several scenarios of multiple T cell clones responding to the same target at once. Each T cell clone is characterized by its reactivity to target antigen, p_i , and its initial concentration, $K_i^0(0)$.

Scenario 1. (Five T cell clones, different reactivities). We consider five T cell clones that differ only in terms of their reactivities to the target antigen. For $i = 1, \dots, 5$ we set reactivity $\#i$ as $p_i = 2^{-i}$. The initial concentrations are given by $K_i^0(0) = 0.01\text{ k}/\mu\text{L}, \forall i$. We also consider cases of single knockout (SKO),

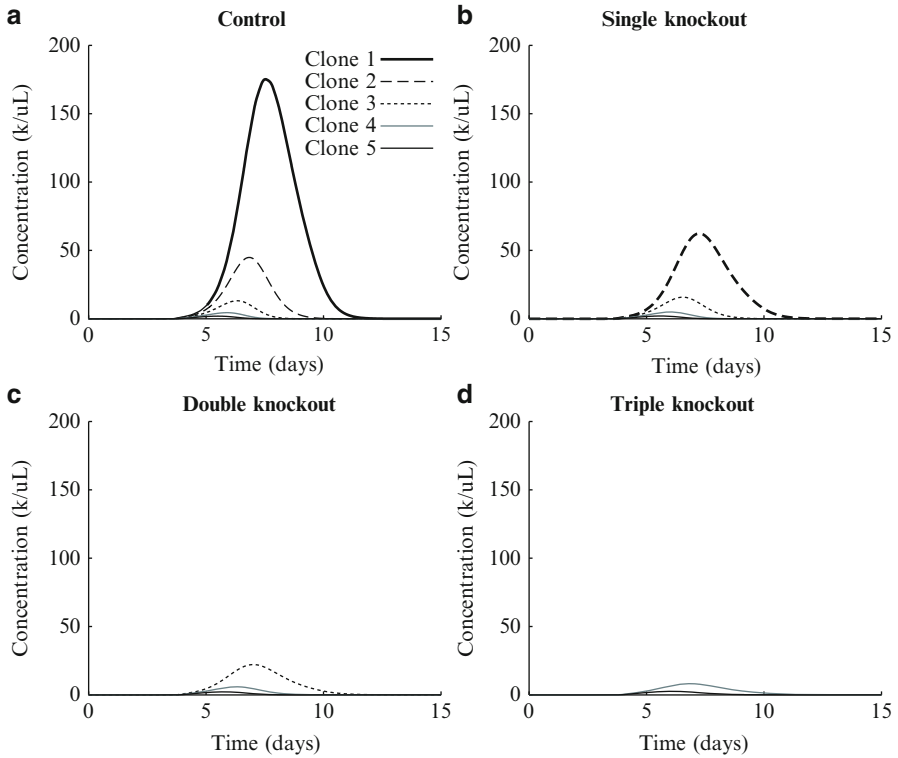


Fig. 6 Basic immunodominance model: time evolution of effector cell clones for Scenario 1. Five T cell clones are present at the same initial concentration $K_i^0(0) = 0.01 \text{ k}/\mu\text{L}$ and reactivities $p_1 = 1/2, p_2 = 1/4, p_3 = 1/8, p_4 = 1/16,$ and $p_5 = 1/32$. All other parameters are taken from Table 1. (a) Control experiment: clones 1–5 all respond. (b) SKO: clone 1 is removed. Only clones 2–5 respond. (c) DKO: clones 1 and 2 are removed. Only clones 3–5 respond. (d) TKO: clones 1–3 are removed. Only clones 4 and 5 respond

double knockout (DKO), and triple knockout (TKO) experiments in which the T cell responses mediated by one, two, or three immunodominant T cell clones are removed. The following cases are considered:

- (a) Control: No T cells are removed. Clones 1–5 all respond.
- (b) SKO: clone 1 is removed. Only clones 2–5 respond.
- (c) DKO: clones 1 and 2 are removed. Only clones 3–5 respond.
- (d) TKO: clones 1–3 are removed. Only clones 4 and 5 respond.

Figure 6 shows the numerical simulations obtained in all four cases. As expected, we see in Fig. 6a that the five T cell clones fall into a hierarchy based on their reactivities. When the dominant clone is removed (a case shown in Fig. 6b), the second most reactive clone partially compensates, i.e., whereas the peak of the response from clone 2 is 44.85 in the control experiment, it rises to 62.39 in the SKO experiment. Similarly, when the two most dominant clones are removed

the third most dominant clone partially compensates (see Fig. 6c) and so on, but the ability of less reactive T cell responses to compensate for more reactive ones decreases rapidly. In the case of the TKO experiment shown in Fig. 6d, the immune response from clone 4 is much weaker than the original immune response generated by clone 1 in the control case shown in Fig. 6a. Our study of Scenario 1 shows that T cell reactivities play a strong role in determining immunodominance hierarchies. Furthermore, less reactive T cell clones have limited ability to compensate for more reactive ones.

The phenomenon of compensation was observed experimentally by van der Most et al. who showed that loss of epitope-specific responses was almost inevitably associated with compensatory responses against subdominant epitopes. In addition, their experiments showed that noticeable compensation by a subdominant response depended on the removal of all or most of the more dominant epitopes, creating room, as it were, for subdominant epitopes to emerge [29]. In the same manner, our simulations show that a response from clone 2 does not substantially emerge until clone 1 is removed and that a response from clone 3 does not emerge until clones 1 and 2 are removed, and so on. By extension, a response against a subdominant epitope is likely not to emerge until all or most T cell clones, specific for the dominant epitope (or epitopes), are removed. The degrees of shift in hierarchy become more prominent in the following examples.

Scenario 2. (Four clones, different initial concentrations). We consider four T cell clones with the same reactivities. These clones differ only in their initial concentrations. In this case, the reactivities are set as $p_i = 1/2$, $i = 1, \dots, 4$. The initial concentrations are taken as: $K_1^0(0) = 0.04$ k/ μ L, $K_2^0(0) = 0.01$ k/ μ L, $K_3^0(0) = 2.5 \times 10^{-3}$ k/ μ L, $K_4^0(0) = 6.25 \times 10^{-4}$ k/ μ L. As before, we consider SKO, DKO, and TKO experiments. Figure 7 shows the results of the numerical simulations.

Figure 7a shows that the four T cell clones fall into a hierarchy based on their initial concentrations. Specifically, the T cell response of clone 1 starts and remains exactly four times higher than that of clone 2. Likewise, the response of clone 2 starts and remains exactly four times higher than that of clone 3, and so on. Since the reactivities p_i are identical for all four clones, the equations determined by Eqs. (15)–(19) for each clone are also identical, meaning that the four T cell responses fall into a linear relation determined by their initial conditions.

When the dominant clone is removed, the second most frequent clone compensates effectively, even though it starts with an initial concentration that is four times less than that of clone 1 (see Fig. 7b). Indeed, the T cell response for clone 2 more than doubles between the control and SKO experiments. Similarly, when the two most dominant clones are removed the third most frequent clone also compensates effectively and so on (see Fig. 6c, d).

Scenario 3. (Two clones, one with a higher reactivity and one with a higher precursor concentration). In Scenarios 1 and 2, we examined the effects of varying reactivities and initial concentrations separately. In this case we vary both parameters and consider two clones. We start by considering a possible

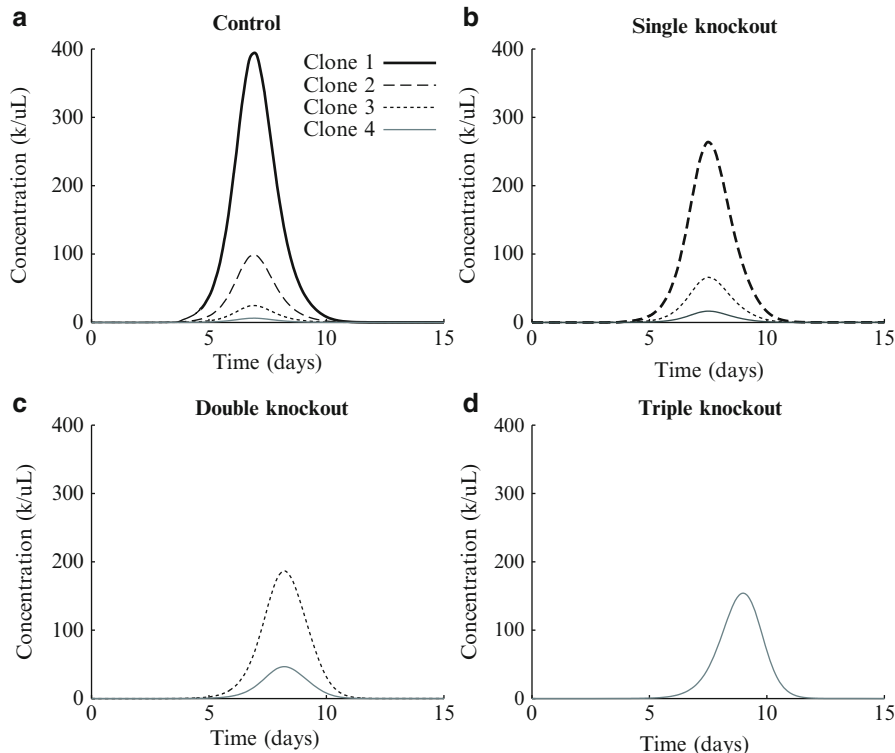


Fig. 7 Basic immunodominance model: time evolution of effector cell populations for Scenario 2. Four T cell clones are present with the same reactivity $p_i = 1/2$ and initial concentrations $K_1^0(0) = 0.04$, $K_2^0(0) = 0.01$, $K_3^0(0) = 2.5 \times 10^{-3}$, and $K_4^0(0) = 6.25 \times 10^{-4}$ k/ μ L. All other parameters are taken from Table 1. (a) Control experiment: clones 1–4 all respond. (b) SKO: clone 1 is removed. Only clones 2–4 respond. (c) DKO: clones 1 and 2 are removed. Only clones 3 and 4 respond. (d) TKO: clones 1–3 are removed. Only clone 4 responds

primary response in which the more reactive clone starts at a lower concentration than the less reactive clone. For our hypothetical secondary response, the initial concentrations are reversed.

1. Reactivity: $p_1 = 1/2$
 Initial concentration: $K_1^0(0) = 0.004$ (primary), 0.04 (secondary) k/ μ L
2. Reactivity: $p_2 = 1/4$
 Initial concentration: $K_2^0(0) = 0.04$ (primary), 0.004 (secondary) k/ μ L

Figure 8 shows numerical solutions for Scenario 3. In Fig. 8a we see that the clone with the higher initial concentration dominates during the primary response. Indeed, clone 2 produces a response that is about three times as high as the response of clone 1. However, by day 10, the population of clone 1 persists whereas the population of clone 2 has nearly vanished. The more reactive clone,

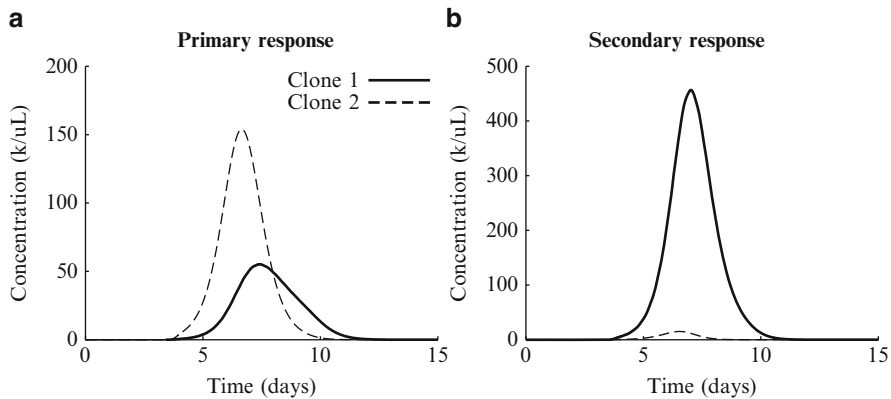


Fig. 8 Basic immunodominance model: time evolution of effector cell populations for Scenario 3. **(a)** Primary response. The less reactive clone is more common. Initial concentrations for the two clones are $K_1^0(0) = 0.004$ and $K_2^0(0) = 0.04$ k/ μ L. **(b)** Secondary response. The two clones have switched places, and now the more reactive clone is more common. Initial concentrations for the two clones are $K_1^0(0) = 0.04$ and $K_2^0(0) = 0.004$ k/ μ L. All other parameters are taken from Table 1

clone 1, ends up producing a more long-lived T cell response than clone 2, and so it follows that this clone might also end up producing a greater number of memory T cells and hence a stronger secondary response. For now, we leave the explicit modeling of memory T cell formation for a future work. Nonetheless, we see from Fig. 8a that iTreg-mediated contraction could give rise to a natural process of “collective affinity maturation” that enables the memory repertoire to select for highly reactive clones even when these clones do not produce the most dominant primary responses.

Without explicitly modeling memory T cell formation, let us suppose that between primary and secondary responses, the composition of the T cell repertoire shifts in favor of the more reactive T cell clone. In particular, suppose that for the hypothetical secondary response, the initial concentrations are reversed. Then, Fig. 8b shows that clone 1 clearly dominates the secondary response. Furthermore, both primary and secondary responses start with the same total initial concentration of T cells, but a much stronger response from clone 1 causes the combined secondary response to peak at over twice the height of the combined primary response.

For simplicity, we generated a hypothetical secondary response by switching the initial concentrations of the two T cell populations, but there is no reason to assume that initial concentrations must switch or that the total initial population must stay the same. In fact, the memory pool generated after a primary response is probably larger than the original naïve T cell pool. Yet even with this simplified view of collective affinity maturation, we see that simple shifts in the relative distribution of T cell clones may result in large differences in subsequent responses. Hence, a mechanism of immunodominance mediated by iTregs may serve as a global,

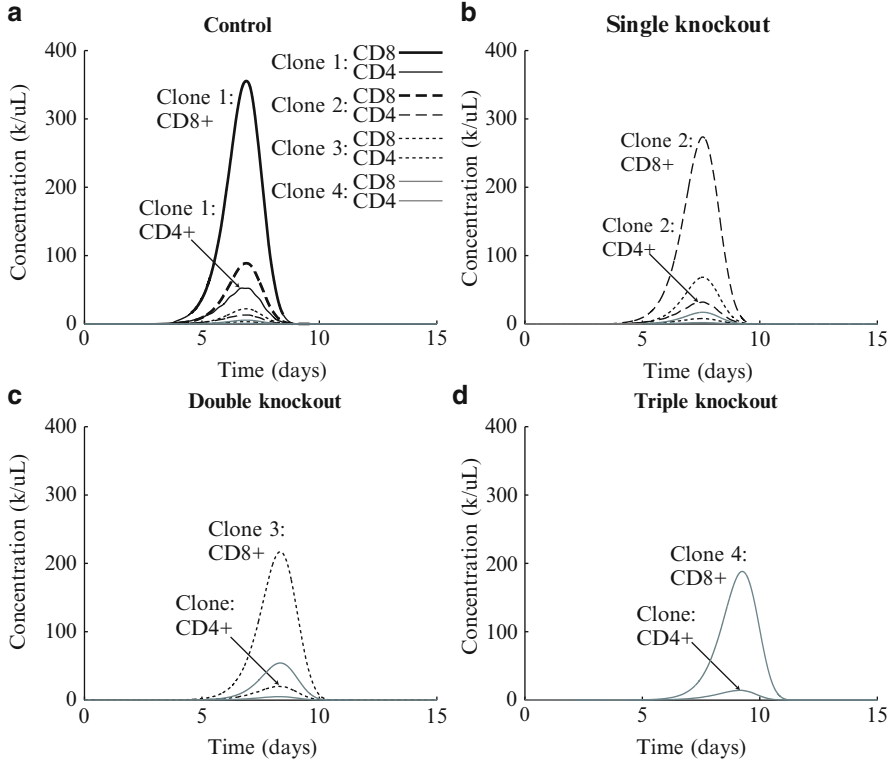


Fig. 9 Extended immunodominance model: time evolution of effector cell populations for Scenario 2. Four T cell clones are present with the same reactivity $p_i = 1/2$ and initial naïve CD8+ concentrations $K_1^0(0) = 0.04$, $K_2^0(0) = 0.01$, $K_3^0(0) = 2.5 \times 10^{-3}$, and $K_4^0(0) = 6.25 \times 10^{-4}$ k/ μ L. Initial naïve CD4+ concentrations are given by $H_i^0(0) = 1.5K_i^0(0)$. Parameters that are not listed in Table 2 are taken from Table 1. (a) Control experiment: clones 1–4 all respond. (b) SKO: clone 1 is removed. Only clones 2–4 respond. (c) DKO: clones 1 and 2 are removed. Only clones 3 and 4 respond. (d) TKO: clones 1–3 are removed. Only clone 4 responds

self-organizing phenomenon among simultaneous T cell responses that serves to improve the overall quality (rather than just the quantity) of the T cell repertoire.

To compare with the basic model Eqs. (1) and (2), we simulate *Scenario 2* from Sect. 4 with the extended model Eqs. (7)–(14). Following Scenario 2 of the basic model, we consider four T cell clones with the same reactivities that only differ in terms of their initial concentrations. All reactivities are assumed to be identical: $p_i = 1/2$, $i = 1, \dots, 4$, and the initial concentrations of naïve CD8+ cells are taken as: $K_1^0(0) = 0.04$ k/ μ L, $K_2^0(0) = 0.01$ k/ μ L, $K_3^0(0) = 2.5 \times 10^{-3}$ k/ μ L, and $K_4^0(0) = 6.25 \times 10^{-4}$ k/ μ L. For each clone, the initial concentrations of naïve CD4+ cells are taken to be $H_i^0(0) = 1.5K_i^0(0)$, which is a typical observed proportion of CD4+ and CD8+ T cells [5].

The results of the simulation are shown in Fig. 9. In Fig. 9a we see that the four T cell clones fall into a hierarchy based on their initial concentrations. When the

dominant clone is removed, the second most frequent clone compensates effectively, even though it starts with an initial concentration that is four times less than that of clone 1 (see Fig. 9b). In addition, when the two most dominant clones are removed the third most frequent clone also compensates effectively, and so on (see Fig. 9c, d).

From Figs. 9 and 7, we see that the qualitative behavior of immunodominance seen in the basic model is preserved in the extended model, which explicitly incorporates separate CD4+ and CD8+ T cell dynamics. The basic model allows us to focus on the role of negative feedback between effector and regulatory T cells in producing immunodominance. The extended model captures more biologically accurate dynamics. However, it requires more comprehensive parameter estimates and more extensive analysis. The overall characteristics of both models are similar.

5 Conclusion and Discussion

In this chapter we provided an overview of our mathematical models for the regulation of the primary T cell response and of immunodominance. Our mathematical models were constructed based on a set of basic principles. A robust T cell contraction was shown to emerge as a result of an adaptive regulatory mechanism. We also showed that immunodominance may occur as a natural consequence of iTreg-mediated T cell contraction. For both problems, we provided a basic model that does not include helper T cells and an extended model that includes the helper T cells. Our numerical simulations focused on the immunodominance models. The simulations showed that the qualitative behavior of the simple and of the extended models is identical.

The main point that we emphasized throughout the chapter is that the modeling of these biological phenomena should focus on the basic principles that control the emerging dynamics. While it is desirable that the mathematical models accurately capture the main biological ingredients, certain simplifications allow us to focus on the basic principles. A basic model that captures the desirable qualitative features can be always extended later on to reflect more accurate biology. This was the methodology we followed when developing these models.

Our models do not take into account the suppression of APCs by iTregs, although it is a known function of regulatory T cells [6]. Incorporating suppression of APCs is a direction for a future work and may partly explain why competition is only observed for epitopes presented on the same APC. In this light, considering spatial elements is another relevant extension, since regulatory T cells locally suppress cells in a contact-dependent manner, but no longer inhibit cells that have moved out of the vicinity [28]. In the context of immunodominance, regulatory (or suppressor) T cells give rise to highly localized inhibition that operates only in the context of one or a few common APCs [26]. In their mathematical models, León et al. assume that regulatory and effector cells need to be activated by APCs that are close in space and time in order to interact [18, 19]. Indeed, such localization may be necessary to prevent a regulatory response from shutting down the whole immune system.

One of the consequences of our work is that immunodominance provides a means of peripheral positive selection that may be optimal in most circumstances, since it generates highly adapted responses against specifically targeted antigens (a response that targets the most reactive clones). Such a pattern must be disadvantageous against rapidly evolving pathogens such as HIV or cancer that can evade narrow T cell responses. Hence, our model of iTreg-mediated immunodominance may have implications for improving therapy via T cell vaccinations. In particular, our model suggests a possible negative correlation between immunodominance, driven by contraction, and epitope spread, driven by expansion. In this case, the strength and timing of the iTreg response may cause a shift in T cell dynamics toward a narrower or broader response, i.e., toward immunodominance or epitope spread. From these results, we hypothesize that temporarily suppressing the de novo generation of iTregs following T cell vaccination may result in a broader T cell response than normal against multiple target epitopes, which will then make it more likely for the immune system to eliminate rapidly evolving targets that would otherwise escape immune detection.

Acknowledgements This work was supported in part by the joint NSF/NIGMS program under Grant Number DMS-0758374 and in part by Grant Number R01CA130 817 from the National Cancer Institute. The content is solely the responsibility of the authors and does not necessarily represent the official views of the National Cancer Institute or the National Institutes of Health.

References

1. Antia, R., Bergstrom, C.T., Pilyugin, S.S., Kaech, S.M., Ahmed, R.: Models of CD8+ responses: 1. What is the antigen-independent proliferation program. *J. Theor. Biol.* **221**(4), 585–598 (2003)
2. Badovinac, V.P., Haring, J.S., Harty, J.T.: Initial T cell receptor transgenic cell precursor frequency dictates critical aspects of the CD8(+) T cell response to infection. *Immunity* **26**(6), 827–841 (2007)
3. Belz, G.T., Zhang, L., Lay, M.D., Kupresanin, F., Davenport, M.P.: Killer T cells regulate antigen presentation for early expansion of memory, but not naïve, CD8+ T cell. *Proc. Natl. Acad. Sci. USA* **104**(15), 6341–6346 (2007)
4. Borghans, J.A., Taams, L.S., Wauben, M.H., de Boer, R.J.: Competition for antigenic sites during T cell proliferation: A mathematical interpretation of in vitro data. *Proc. Natl. Acad. Sci. USA* **96**(19), 10782–10787 (1999)
5. Catron, D.M., Itano, A.A., Pape, K.A., Mueller, D.L., Jenkins, M.K.: Visualizing the first 50 hr of the primary immune response to a soluble antigen. *Immunity* **21**(3), 341–347 (2004)
6. Chang, C.C., Ciubotariu, R., Manavalan, J.S., Yuan, J., Colovai, A.I., Piazza, F., Lederman, S., Colonna, M., Cortesini, R., Dalla-Favera, R., Suci-Foca, N.: Tolerization of dendritic cells by T(S) cells: The crucial role of inhibitory receptors ILT3 and ILT4. *Nat. Immunol.* **3**(3), 237–243 (2002)
7. De Boer, R.J., Perelson, A.S.: T cell repertoires and competitive exclusion. *J. Theor. Biol.* **169**(4), 375–390 (1994)
8. De Boer, R.J., Perelson, A.S.: Toward a general function describing T cell proliferation. *J. Theor. Biol.* **175**(4), 567–576 (1995)

9. De Boer, R.J., Homann, D., Perelson, A.S.: Different dynamics of CD4+ and CD8+ T cell responses during and after acute lymphocytic choriomeningitis virus infection. *J. Immunol.* **171**(8), 3928–3935 (2003)
10. De Boer, R.J., Oprea, M., Antia, R., Murali-Krishna, K., Ahmed, R., Perelson, A.S.: Recruitment times, proliferation, and apoptosis rates during the CD8(+) T-cell response to lymphocytic choriomeningitis virus. *J. Virol.* **75**, 10663–10669 (2001)
11. Grufman, P., Wolpert, E.Z., Sandberg, J.K., Karre, K.: T cell competition for the antigen-presenting cell as a model for immunodominance in the cytotoxic T lymphocyte response against minor histocompatibility antigens. *Eur. J. Immunol.* **29**(7), 2197–2204 (1999)
12. Handel, A., Antia, R.: A simple mathematical model helps to explain the immunodominance of CD8 T cells in influenza A virus infections. *J. Virol.* **82**(16), 7768–7772 (2008)
13. Kaech, S.M., Ahmed, R.: Memory CD8+ T cell differentiation: Initial antigen encounter triggers a developmental program in naïve cells. *Nat. Immunol.* **2**(5), 415–422 (2001)
14. Kedl, R.M., Kappler, J.W., Marrack, P.: Epitope dominance, competition and T cell affinity maturation. *Curr. Opin. Immunol.* **15**(1), 120–127 (2003)
15. Kedl, R.M., Rees, W.A., Hildeman, D.A., Schaefer, B., Mitchell, T., Kappler, J., Marrack, P.: T cells compete for access to antigen-bearing antigen-presenting cells. *J. Exp. Med.* **192**(8), 1105–1113 (2000)
16. Kim, P.S., Lee, P.P., Levy, D.: A theory of immunodominance and adaptive regulation. *Bull. Math. Biol.* **73**, 1645–1665 (2011)
17. Kim, P.S., Lee, P.P., Levy, D.: Emergent group dynamics governed by regulatory cells produce a robust primary T cell response. *Bull. Math. Biol.* **72**, 611–644 (2010)
18. León, K., Lage, A., Carneiro, J.: How regulatory CD25+CD4+ T cells impinge on tumor immunobiology? On the existence of two alternative dynamical classes of tumors. *J. Theor. Biol.* **247**(1), 122–137 (2007)
19. León, K., Lage, A., Carneiro, J.: How regulatory CD25+CD4+ T cells impinge on tumor immunobiology: The differential response of tumors to therapies. *J. Immunol.* **179**(9), 5659–5668 (2007)
20. Mercado, R., Vijh, S., Allen, S.E., Kerksiek, K., Pilip, I.M., Pamer, E.G.: Early programming of T cell populations responding to bacterial infection. *J. Immunol.* **165**(12), 6833–6839 (2000)
21. Nowak, M.A.: Immune responses against multiple epitopes: A theory for immunodominance and antigenic variation. *Semin. Virol.* **7**, 83–92 (1996)
22. Probst, H.C., Dumrese, T., van den Broek, M.F.: Cutting edge: Competition for APC by CTLs of different specificities is not functionally important during induction of antiviral responses. *J. Immunol.* **168**(11), 5387–5391 (2002)
23. Roy-Proulx, G., Meunier, M.C., Lanteigne, A.M., Brochu, S., Perreault, C.: Immunodominance results from functional differences between competing CTL. *Eur. J. Immunol.* **31**(8), 2284–2292 (2001)
24. Sakaguchi, S., Yamaguchi, T., Nomura, T., Ono, M.: Regulatory t cells and immune tolerance. *Cell* **133**(5), 775–787 (2008)
25. Scherer, A., Bonhoeffer, S.: Epitope down-modulation as a mechanism for the coexistence of competing T-cells. *J. Theor. Biol.* **233**(3), 379–390 (2005)
26. Sercarz, E.E., Lehmann, P.V., Ametani, A., Benichou, G., Miller, A., Moudgil, K.: Dominance and crypticity of T cell antigenic determinants. *Annu. Rev. Immunol.* **11**, 729–766 (1993)
27. Scherer, A., Salathé, M., Bonhoeffer, S.: High epitope expression levels increase competition between T cells. *PLoS Comput. Biol.* **2**(8), e109 (2006)
28. Trimble, L.A., Lieberman, J.: Circulating CD8 T lymphocytes in human immunodeficiency virus-infected individuals have impaired function and downmodulate CD3 zeta, the signalling chain of the T-cell receptor complex. *Blood* **91**(2), 585–594 (1998)
29. van der Most, R.G., Murali-Krishna, K., Lanier, J.G., Wherry, E.J., Puglielli, M.T., Blattman, J.N., Sette, A., Ahmed, R.: Changing immunodominance patterns in antiviral CD8 T-cell responses after loss of epitope presentation or chronic antigenic stimulation. *Virology* **315**(1), 93–102 (2003)

30. van Stipdonk, M.J., Hardenberg, G., Bijker, M.S., Lemmens, E.E., Droin, N.M., Green, D.R., Schoenberger, S.P.: Dynamic programming of CD8+ T lymphocyte responses. *Nat. Immunol.* **4**(4), 361–365 (2003)
31. van Stipdonk, M.J., Lemmens, E.E., Schoenberger, S.P.: Naïve CTLs require a single brief period of antigenic stimulation for clonal expansion and differentiation. *Nat. Immunol.* **2**(5), 423–429 (2001)
32. Wodarz, D., Thomsen, A.R.: Effect of the CTL proliferation program on virus dynamics. *Int. Immunol.* **17**(9), 1269–1276 (2005)
33. Yang, Y., Kim, D., Fathman, C.G.: Regulation of programmed cell death following T cell activation in vivo. *Int. Immunol.* **10**(2), 175–183 (1998)



<http://www.springer.com/978-1-4614-4177-9>

Mathematical Methods and Models in Biomedicine

Ledzewicz, U.; Schättler, H.; Friedman, A.; Kashdan, E.

(Eds.)

2013, XI, 427 p. 94 illus., Softcover

ISBN: 978-1-4614-4177-9